Int. J. Heat Mass Transfer. Vol. 20, pp. 141–151 Pergamon Press 1977 Printed in Great Britain

EDDY DIFFUSIVITY OF HEAT TRANSFER IN THE RADIAL DIRECTION FOR TURBULENT FLOW OF MERCURY IN ANNULI*

O. E. DWYER, P. J. HLAVAC† and B. G. NIMMO‡
Brookhaven National Laboratory, Upton, NY 11973, U.S.A.

(*Received 22 September 1975 and in revised form 20 April 1976*)

Abstract—A basic experimental study of the fluid dynamics and heat-transfer characteristics of mercury, in fully developed turbulent flow through annuli, was carried out. This paper, the third in a series on this project, presents the results on the eddy diffusivity of heat transfer. Velocity and temperature profiles were measured in vertical annuli with heat transfer from the inner wall only, and experiments were conducted where the mercury either did not wet at all, or did thoroughly wet, the channel walls.

The shapes of the ε_H profiles were found to be similar to those of the ε_M profiles, with the maxima and minima often occurring at or near the same radial locations, for the same experimental conditions. All minima occurred at the radius of maximum velocity, but the valleys in ε_H profiles were relatively more shallow than those in the ε_M profiles. The effect of wetting on the relative shape of the ε_H profile, as in the case of the ε_M profile, was found to be appreciable. When both walls were unwetted, the hydrodynamic behavior of the mercury was found [1] to be very similar to that of ordinary fluids. Although the present results obtained with unwetted walls do not agree with predictions based on existing theory, they do lend appreciable support to the method of Ramm and Johannsen [7].

NOMENCLATURE

- C_p, specific heat [J/(kg °C)];
- D_e, $2(r_2-r_1)$ = equivalent diameter [m];
- k, molecular thermal conductivity [W/(m °C)];
- k_e, eddy thermal conductivity [W/(m °C)];
- L_h, heated length [m];
- Pr, $= C_p\mu/k$, Prandtl number [dimensionless];
- q, heat flux at radial distance r [W/m^2];
- Q, heater power [W];
- q_1, heat flux at inner wall [W/m^2];
- r, radial distance [cm or m];
- r_1, r_2, inner and outer radii, respectively, of annulus [cm or m];
- r_m, radius of maximum time-average velocity [m];
- Re, $D_e v_a \rho/\mu$ = Reynolds number [dimensionless];
- t, time-average value of temperature at r [°C];
- t_{in}, inlet temperature [°C];
- v, local time-mean velocity at radial distance r [m/s];
- v_a, $\left[2\int_{r_1}^{r_2} vr\,dr\right]\Big/[r_2^2-r_1^2]$ = average value of v across distance (r_2-r_1) [m/s];
- x, axial distance [m].

Greek symbols

- α, $k/\rho C_p$ = molecular diffusivity of heat transfer [m^2/s];
- ε_H, $k_e/\rho C_p$ = eddy diffusivity of heat transfer at radial distance r [m^2/s];
- $\varepsilon_{H1}, \varepsilon_{H2}$, same as ε_H except for inner and outer portions, respectively, of annulus [m^2/s];
- $(\varepsilon_{H1})_{max}, (\varepsilon_{H2})_{max}$, maximum values of ε_{H1} and ε_{H2}, respectively;
- ε_M, eddy diffusivity of momentum transfer at radial distance r [m^2/s];
- μ, viscosity [kg/(m s)];
- ν, μ/ρ = kinematic viscosity [m^2/s];
- ρ, density [kg/m^3];
- $\bar{\psi}$, effective average value of $\varepsilon_H/\varepsilon_M$ for use in heat-transfer correlations for turbulent channel flow [see equations (7)] [dimensionless];
- $\bar{\psi}_1$, effective average value of $\varepsilon_H/\varepsilon_M$ in inner portion of annulus, used for estimating heat-transfer coefficients where heat is transferred from the inner wall only [dimensionless].

1. INTRODUCTION

THIS paper is the third in a series of four, all of which are based on a fundamental study of the fluid dynamics and heat transfer for turbulent flow of mercury in smooth concentric annuli. Heat was transferred from the inner wall only, the heat flux was uniform in all directions, and the outer wall was adiabatic. Special attention was given to the effects of wetting vs non-wetting on the various results. Data were taken only under fully developed flow and heat-transfer conditions. The fluid dynamics results, consisting of velocity

*This work was performed under the auspices of the U.S. Energy Research and Development Administration.

†Present address: Allied Maintenance Corp., Aviation Fuel Division, 2 Pennsylvania Plaza, New York, NY 10001, U.S.A.

‡Present address: Associate Professor, Dept. of Mech. Engng and Aerospace Sciences, College of Engineering, Florida Technological University, Orlando, FL 32816, U.S.A.

profiles, radii of maximum velocity, and eddy diffusivities of momentum transfer are given in [1]. The friction factor results are given in [2].

The main purpose of this paper is to present the results of the temperature-profile measurements in terms of the radial eddy diffusivities of heat transfer. Besides the time–mean radial temperature distribution, the following measurements were made: time–mean surface temperatures of the heater, time–mean velocity profiles, flow rate, and inlet and outlet stream temperatures.

2. EXPERIMENTAL

The equipment is described in considerable detail in [1]. The experiments were carried out in a recirculation loop built of stainless-steel pipe. The mercury flowed vertically downward through the test section.

2.1. *Test sections*

Basically, a test section consisted of a long stainless-steel pipe in which an electrical rod heater was concentrically fixed [1]. Three different test sections were used. They had r_2/r_1 ratios of 2.09 ($r_1 = 1.065$ cm, $r_2 = 2.222$ cm), 2.78 ($r_1 = 0.635$ cm, $r_2 = 1.764$ cm), and 4.00 ($r_1 = 0.556$ cm, $r_2 = 2.222$ cm). Each test section had three so-called traversing stations—*A*, *B* and *C*. At each traversing station there were three pressure taps, two velocity probes, and one temperature probe. The three probes were 120° apart, and the three pressure taps were located midway between adjacent probe seals. All the experimental results given in this paper were obtained at traversing station *A*, whose axial location corresponded to 127, 79 and 88 equivalent diameters from the flow inlet point, for radius ratios of 2.09, 2.78 and 4.00, respectively. Measurements made at station *B*, which corresponded to 95, 58 and 66 equivalent diameters for radius ratios of 2.09, 2.78 and 4.00, respectively, indicated that fully developed flow and thermal conditions were well established at traversing station *A*.

The probe seals allowed a 3.2-mm-dia rod to be accurately moved in and out without mercury leakage. The temperature probes consisted of copper–constantan thermocouples mounted in streamlined stainless-steel support rods. The thermocouples were stainless-steel sheathed, had an outside diameter of 0.50 mm, contained compacted MgO electrical insulation, and were grounded. The sensing tip of each temperature probe was located 6.4 mm upstream from the support rod, that is, the thermocouple tip made a 90-degree angle with the rod. The tip approached each wall of the annulus to within ~0.4 mm. The maximum thickness of the streamlined support rod "seen" by the flowing mercury was ~1.0 mm. The radial location of the thermocouple junction, which was determined by means of a vernier scale, was estimated to be accurate to ±0.025 mm.

2.2. *Rod heaters*

The heaters, made especially for the study, consisted of a Nichrome coil in MgO insulation and swaged in a copper tube having a 2.55-mm-thick wall. Copper-sheathed copper–constantan thermocouples were imbedded (axially) slightly below the test element surface for measuring heating-wall temperatures. The thermocouple junctions were grounded and located just at the surface of the copper cladding. The procedure for putting the sheathed thermocouples in the rod wall is given in Ref. [3]. The I.D. and O.D. of the thermocouple sheaths were ~0.36 and ~0.50 mm, respectively.

In the first test section used ($r_2/r_1 = 2.78$), there were nine thermocouples placed in each heater rod, 40° apart on the circumference. Three (120° apart) each were located at traversing stations *A*, *B* and *C*. In the last two sections (2.09 and 4.00), there were six thermocouples in each heater, 60° apart, three each at stations *A* and *B*.

After the thermocouples were imbedded, and the surface smoothed and made perfectly cylindrical, a 0.025-mm-thick layer of nickel was electroplated on the rod. This was followed by a final 0.010-mm-thick electroplate of copper, if a wetting surface was desired, or by a final 0.0025-mm-thick plate of chromium, if a nonwetting surface was desired. In the former case, the copper flash coating was soon dissolved away by the mercury, exposing a completely wetted nickel surface. The nonwetted heaters usually lasted a few months before the mercury penetrated the chromium layer and damaged the thermocouple junctions, while the wetted heaters lasted only two to three weeks. All heaters were X-rayed to make sure that only those with concentrically located Nichrome coils were used. Each heater was also carefully checked for straightness, and straightened if necessary, before use. Before insertion in the test section, each heater was cleaned with detergent, rinsed with water, rinsed with acetone, and wiped dry with pure unspun cotton.

The heater rods were held firmly at the bottom of the test section; a tube-sheet bellows assembly at the top of the test section accommodated differences in thermal expansion between the heater rod and the surrounding pipe.

2.3. *Experimental procedures*

Before each series of tests, the mercury was circulated isothermally through the loop, and the heater thermocouples and the probe thermocouple were checked against the inlet temperature to the test section. This temperature was determined from a calibrated copper–constantan thermocouple in a thermowell in the well mixed inlet mercury stream. Power was then gradually applied up to the desired level and the flow rate was established. The cooling water rate to the heat exchanger was controlled to maintain the desired temperature level and the magnitude of the inlet temperature to the test section.

When the steady-state operating conditions were established, the flow rate, power level, and inlet, outlet, and surface temperatures were recorded. The surface-temperature thermocouples and the probe thermocouples were bucked against the inlet temperature, which tended to cancel out the effects of any slight

variations of the inlet temperature on the thermal data. When a temperature traverse was made, all probes but the one in use were backed out to within 0.50 mm of the outer wall. The temperature at a given radial position, relative to the inlet temperature, was traced (in terms of millivolts) on a recorder chart over a period of 20–60 s. The thermocouples and the recording system were sufficiently sensitive to pick up fluctuations due to stream turbulence. These fluctuations were a maximum at a short distance from the inner wall, where the effects of the temperature and velocity profiles were maximized. The amplitude of these fluctuations became negligible as the inner wall was closely approached and as the outer wall was more remotely approached. The fluctuations also decreased as the flow rate was increased; but, as one would expect, they increased with increase in heat flux. For a given radial position, the local stream temperature was taken as the time-average value.

The temperature profile for a given set of conditions was based on the data points taken during three or four consecutive temperature traverses. As shown by the typical results shown in Fig. 1, data reproducibility was quite satisfactory. Some profile-temperature data showed slightly less scatter, while some showed slightly more.

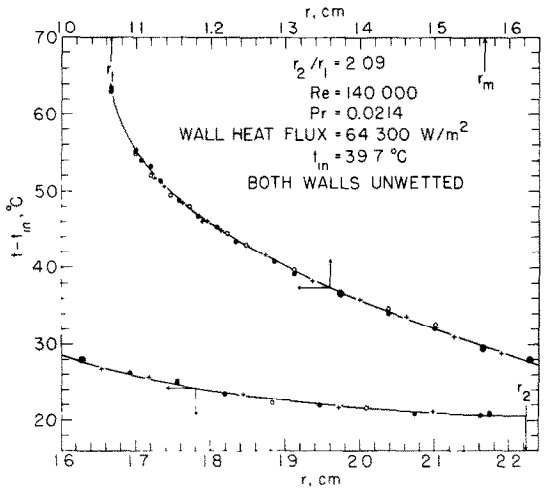

FIG. 1. Radial distribution of typical time-mean local temperature readings. The three different symbols represent three different temperature traverses.

3. METHOD OF CALCULATING EDDY DIFFUSIVITIES OF HEAT TRANSFER FROM THE DATA

For the situation of heat transfer from the inner wall of an annulus, the eddy diffusivity of heat transfer, ε_H, at any radial distance r is defined by the equation

$$\frac{q}{\rho C_p} = (\alpha + \varepsilon_H)\left(-\frac{dt}{dr}\right). \tag{1}$$

The other symbols are defined in the Nomenclature. Since the heat transferred across an imaginary cylindrical boundary at r is equal to the heat transported away by the mercury flowing between r and r_2, we can write the heat-balance equation

$$2\pi r q = 2\pi C_p \rho \frac{dt}{dx}\int_r^{r_2} v r\, dr. \tag{2}$$

We can write an analogous equation for the heat transferred at the heating surface, i.e.

$$2\pi r_1 q_1 = \pi(r_2^2 - r_1^2) v_a C_p \rho \frac{dt}{dx}. \tag{3}$$

Dividing equation (2) by equation (3), and solving for q, gives

$$q = \frac{2q_1 r_1 \int_r^{r_2} v r\, dr}{r v_a (r_2^2 - r_1^2)}, \tag{4}$$

where q_1 is given by

$$q_1 = \frac{Q}{2\pi r_1 L_h}. \tag{5}$$

Substituting q_1 from equation (5) into equation (4), then substituting the resulting expression for q into equation (1), then solving for ε_H, and then dividing both sides of the resulting equation by α, we finally obtain

$$\frac{\varepsilon_H}{\alpha} = \frac{Q\int_r^{r_2} v r\, dr}{\pi v_a L_h k (r_2^2 - r_1^2) r\left(-\frac{dt}{dr}\right)} - 1, \tag{6}$$

which is the equation that we used to calculate the dimensionless eddy diffusivity values shown in Figs. 2–8. In equation (6),

- Q, power input to heater [W];
- v, time-average value of linear velocity at radial distance r [m/s];
- r, radial distance [m];
- v_a, average linear velocity in annulus [m/s];
- L_h, heated length of heater [m];
- k, thermal conductivity of mercury [W/(m °C)];
- r_1, inner radius of annulus [m];
- r_2, outer radius of annulus [m];
- t, time-average value of mercury temperature at r [°C].

In deriving equation (6), it was assumed that k, ρ, and C_p are constants, that is, they do not vary with r, even though the stream temperature varies with r. Actually, these physical properties were evaluated at the average radial temperature. It so happens that they varied very little over the temperature ranges encountered. In the worst case the temperature drop across the annular space was 17°C. Under these conditions, the values of k, ρ and C_p evaluated at the average temperature were within ~0.1, ~1 and 0.2%, respectively, of the limiting values near the walls. These differences are negligible compared to the probable error in the final results.

In calculating ε_H/α by means of equation (6), the values of v were taken as the smoothed values published in [1]. The slopes, dt/dr, of the temperature profile curves were determined graphically by drawing tangents to the curves. These local values were then plotted against r, and a smooth curve drawn through them, as illustrated in Fig. 1. The slopes obtained from these curves are estimated to have an average error of $< 2\%$, which means that the errors in the slopes for a particular curve are most probably due more to the shape of the curve as drawn than to the method of determining the slopes. As the flow rate was varied, the

heat flux at the inner wall was varied to maintain a satisfactory temperature profile across the flow channel. For example, for the set of data presented in Fig. 2, the heat flux varied from 55 100 to 91 800 W/m^2 as the Reynolds number was increased from 96 000 to 383 000.

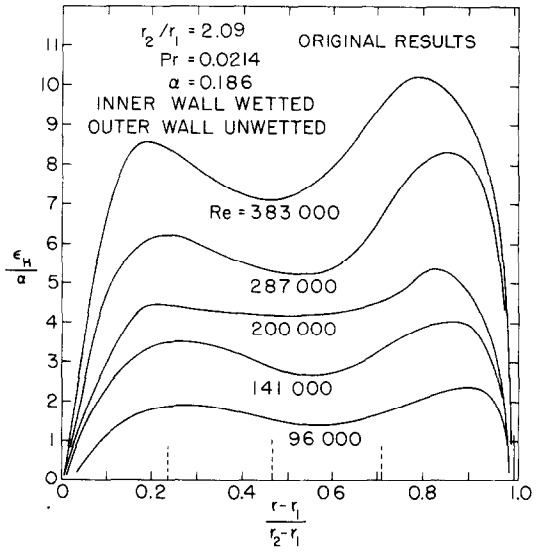

FIG. 2. Radial variation of ε_H/α at different Reynolds numbers for an annulus having the inner wall wetted and the outer wall unwetted. The curves represent original results as calculated by means of equation (6). $r_2/r_1 = 2.09$.

The original values of ε_H/α were finally smoothed and made self-consistent by cross-plotting them against Reynolds number at constant values of r and drawing best-fit curves through the points. It was found that these curves (on log–log plots) for the most part closely approximated straight lines with a slope of 1, indicating that ε_H/α was practically proportional to the Reynolds number.

4. RESULTS

Observed values of ε_H/α are shown in Figs. 2–8. Figure 2 shows the dependence of ε_H/α on radial position and Reynolds number, for the case of $r_2/r_1 = 2.09$ with the inner wall wetted and the outer wall unwetted. The curves in Fig. 2 are referred to as "original results", because they are the curves that were calculated directly from the data. Figure 3 shows the same results after the curves were smoothed by cross-plotting.

As one would expect, the data near the outer wall were considerably less accurate than those at shorter radial distances, because the slope of the t-vs-r curve approaches zero as the outer wall is approached. A very small change in the shape of the temperature–profile curve in this region would therefore produce relatively large changes in the local values of dt/dr. For this reason, the smoothed-results curves always agreed much better with the original-results curves in the inner portion ($r_1 \leqslant r \leqslant r_m$) than in the outer portion ($r_m \leqslant r \leqslant r_2$) of a given annulus. When cross-plotting the original results to obtain the points for the smoothed-results curves, considerable reliance was

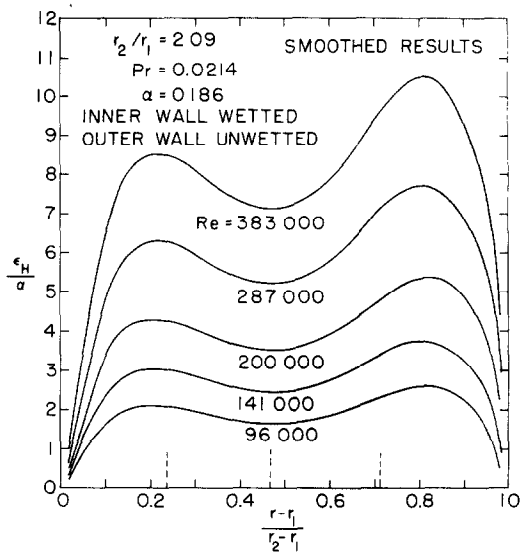

FIG. 3. Same results as in Fig. 2, except they have been smoothed by cross-plotting.

placed on the fact that ε_H/α at a given radial position was essentially proportional to the Reynolds number, and also on the fact that the data in the outer portion of an annulus were more consistent with those in the inner portion at the higher flow rates than at the lower flow rates.

In Figs. 2–8, 10 and 11, three dashed vertical lines appear along the abscissas. The first indicates the radial location of the maximum value of ε_M in the inner portion of the annulus. The second indicates the radial location of r_m, where the velocity profile goes through a maximum and the ε_M profile goes through a minimum. And the third indicates the radial location of the maximum value of ε_M in the outer portion of the annulus. In all the figures, we see that, in the inner portion of the annuli, the maximum values of ε_H and ε_M occur at essentially the same radial location. Also,

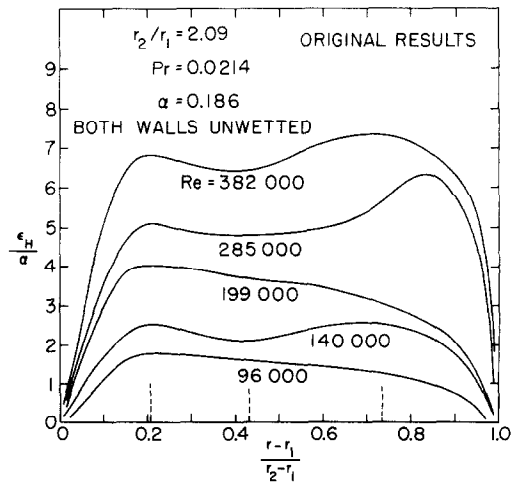

FIG. 4. Radial variation of ε_H/α at different Reynolds numbers for an annulus having both walls unwetted and an r_2/r_1 ratio of 2.09. The curves represent original results as calculated by means of equation (6).

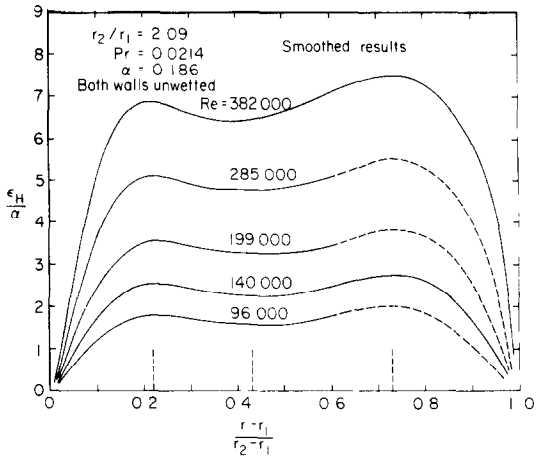

FIG. 5. Same results as in Fig. 4, except they have been smoothed by cross-plotting.

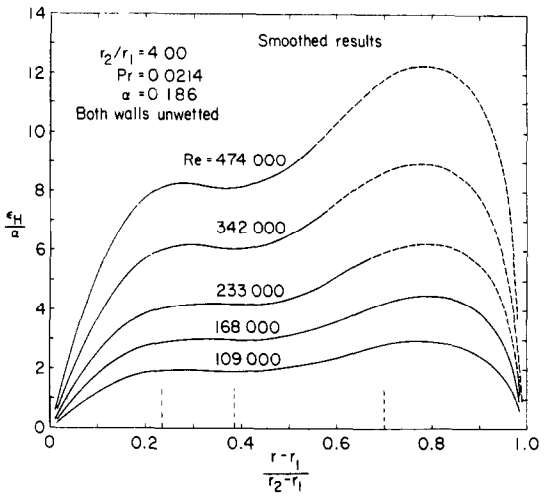

FIG. 6. Radial variation of ε_H/α at different Reynolds numbers for an annulus having both walls unwetted and an r_2/r_1 ratio of 4.00. Smoothed results.

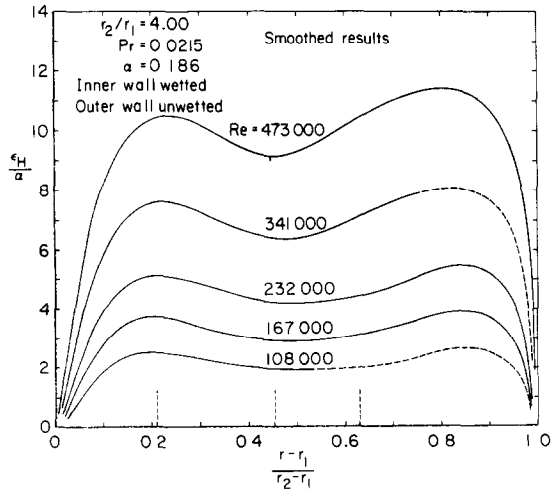

FIG. 7. Radial variation of ε_H/α at different Reynolds numbers for an annulus having the inner wall (only) wetted and an r_2/r_1 ratio of 4.00. Smoothed results.

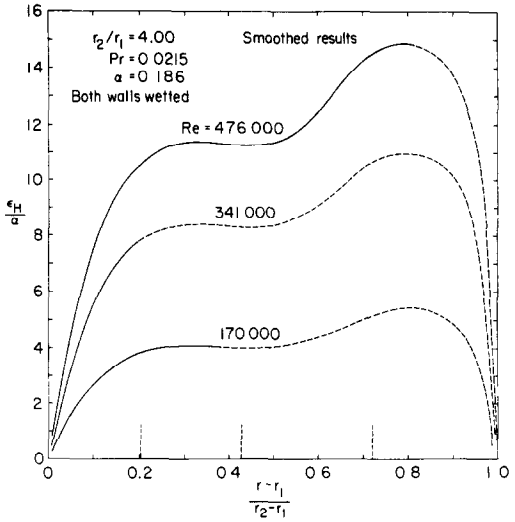

FIG. 8. Radial variation of ε_H/α at different Reynolds numbers for an annulus having both walls wetted and an r_2/r_1 ratio of 4.00. Smoothed results.

we see that at r_m, the ε_H profile also goes through a minimum. In the outer portions of the annuli, we find that the radial location of $(\varepsilon_{H2})_{max}$ generally falls to the right of $(\varepsilon_{M2})_{max}$. We believe that this discrepancy is due to the fact that the ε_H profiles in the radial region near the outer wall are subject to greater error, as already explained.

Figure 4 shows the dependence of ε_H/α on radial position and Reynolds number for the case of $r_2/r_1 = 2.09$ with both walls unwetted. The curves in this figure are original-results curves. Figure 5 presents the same results in the form of "smoothed" curves. Note that in this figure the curves for Reynolds numbers 96 000, 199 000, and 285 000 are drawn dashed in the region near the outer wall. This means that in the ε_H/α-vs-*Re* cross plot, the points for these Reynolds numbers fell appreciably off the curves. This is apparent when comparing the curves for these three Reynolds numbers in Fig. 4 with those in Fig. 5. The discrepancies between Figs. 4 and 5 in the outer portion of the annulus are more or less typical of the present study. Comparisons of Fig. 3 with Fig. 2 and of 5 with 4 give an indication of the accuracy of the present results.

A comparison of Figs. 3 and 5 should show the effect of wetting the inner wall on the shape of the ε_H profile. We see that the ratio $(\varepsilon_{H1})_{max}/(\varepsilon_{H2})_{max}$ in Fig. 3 is appreciably less than in Fig. 5, which theoretically is incorrect. This ratio should be greater in Fig. 3, because, as shown in [1], r_m for the case where the inner wall was wetted was appreciably greater than that for the case where neither wall was wetted. The greater the value of r_m, the greater should be the ratio of the maximum value of ε_H in the inner portion of the annulus to that in the outer portion, other things being as equal as possible. The curves in Fig. 5 appear to be more correct and are consistent with those in Figs. 6–8. No reason can be suggested for the apparently anomalous shapes of the curves in Fig. 3.

In the present study, the first data were taken with the 2.78 annulus. That was before we found that wetting

affected both the velocity and temperature profiles; and, of the five Reynolds numbers used, two temperature profiles were taken with the inner wall wetted, and three with neither wall wetted. The test section was unfortunately replaced before we became aware of the importance of the wetting effect, and so no additional data could be taken. The data taken at the three Reynolds numbers for the condition of both walls unwetted showed too much scatter (for only three Reynolds numbers) for reliable best-fit curves to be drawn through them on the ε_H/α-vs-Re cross plots.

Figures 6–8 show the results obtained with the 4.00 annulus for three different sets of wetting conditions. The results are quite self-consistent, and came much as expected, except for the fact that the curves appear to be too steep near the outer wall. Figure 9 is a normalized plot which compares the curves for the three highest Reynolds numbers in Figs. 6–8. In each case, the minimum value of ε_H falls at the same radial position as the maximum value of v (see Table 2 in [1]).

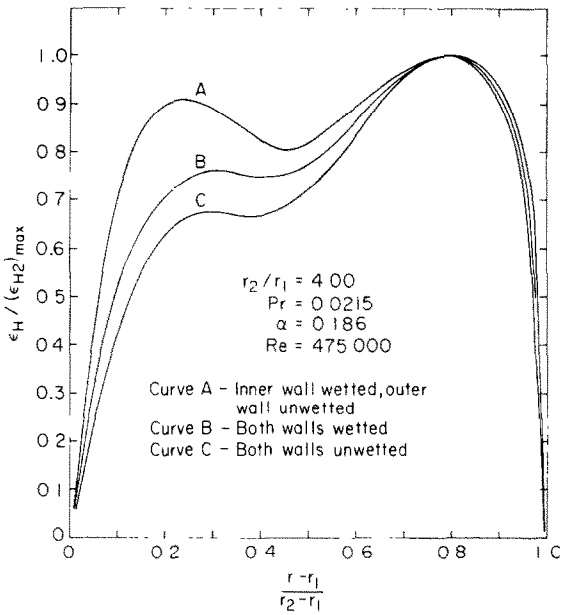

FIG. 9. Normalized plot showing the effect of wetting on radial variation of ε_H for an annulus having an r_2/r_1 ratio of 4.00 and for a Reynolds number of 475 000.

The values of $(r-r_1)/(r_2-r_1)$ at which the minimum values of ε_H occurs are 0.453, 0.432 and 0.380 for curves *A*, *B* and *C*, respectively. As explained in [1], wetting the inner wall produces an extra drag on the liquid which pushes the radius of maximum velocity outward, which, in turn, tends to more equalize both the inner-portion and outer-portion maxima of both the ε_H and ε_M profiles. Thus, we see in Fig. 9 that whereas $(\varepsilon_{H1})_{max}/(\varepsilon_{H2})_{max}$ is only 0.68 for curve *C* (both walls unwetted), it is 0.91 for curve *A* (inner wall wetted, outer wall unwetted). Curve *B* (both walls wetted), as one would expect falls between curves *A* and *B*. It is interesting to note that $(\varepsilon_{H2})_{max}$ for all three cases fell at the same radial position.

Radially local values of ε_M obtained under the same conditions as those under which the ε_H results were obtained are presented in Fig. 10 of [1]. It is therefore possible to calculate radially local values of the ratio $\varepsilon_H/\varepsilon_M$. As already stated the fluid dynamic behavior of the mercury in the cases where both walls were unwetted was very similar to those obtained with ordinary liquids. We can therefore calculate local $\varepsilon_H/\varepsilon_M$ values for radius ratios 2.09 and 4.00 with both walls unwetted and compare the results with theoretically predicted values. Such results for $r_2/r_1 = 2.09$ are presented in Table 1.

With heat transfer from the inner wall, as in the common double-pipe heat exchanger, the temperature gradient is steep near the inner wall and zero at the outer wall, if the outer wall is adiabatic (as in the present study). For this reason, values of the ratio $\varepsilon_H/\varepsilon_M$ need to be known much more accurately in the inner portion of the annulus than in the outer portion. That is why, in Table 1 (and Table 2 also), the radial increments are smaller in the vicinity of the inner wall.

The general magnitude of the results in Table 1 look rather reasonable, except they peak too sharply in the region of r_m. This is caused by the fact that the ε_M values fall rather sharply in this region (see Figs. 12 and 13 in [1]). Table 2 was prepared by dividing the experimentally determined local values of ε_H by the local values of ε_M as predicted by the correlation of Kays and Leung [4]. As seen in Figs. 12 and 13 of [1], this correlation predicts a more shallow valley in the ε_M profile in the region of r_m. The results in Table 2 consequently indicate that the $\varepsilon_H/\varepsilon_M$ profile is rather flat in the turbulent core, which looks more reasonable. As explained earlier, the ε_H results for the inner portion of the annulus are more accurate than those in the outer portion. This will therefore also be true for the results in Tables 1 and 2.

Several years ago, the present senior author published a semi-theoretical equation [5] for predicting the average effective value of $\varepsilon_H/\varepsilon_M$ for use in theoretical equations for predicting Nusselt numbers in channel flow. This equation is

$$\bar{\psi} = [\varepsilon_H/\varepsilon_M]_{ave} = 1 - \frac{1.82}{Pr(\varepsilon_M/\nu)^{1.4}_{max}}. \quad (7)$$

Table 2 shows values of $\bar{\psi}_1$ (i.e. for the inner portion of the annulus) which would be used for predicting the heat-transfer coefficient for heat transfer from the inner wall. These values of $\bar{\psi}_1$ for the five different Reynolds numbers compare quite favorably with the $\varepsilon_H/\varepsilon_M$ values given in the table.

In 1970, Azer [6] published a theoretical method for predicting radially local values of $\varepsilon_H/\varepsilon_M$ for fully developed turbulent flow of liquid metals in concentric annuli.* However, his method predicts quite low results for ε_H (see Figs. 10 and 11) and therefore for $\varepsilon_H/\varepsilon_M$. For example, at a radial distance of $(r-r_1)/(r_2-r_1) = 0.2$, Azer's method predicts $\varepsilon_H/\varepsilon_M$ values of 0.39, 0.44,

*The constant 0.522 in equation (5) of [6] should actually be 0.522b.

Table 1. Experimental values of the ratio $\varepsilon_H/\varepsilon_M$ as a function of Reynolds number and radial distance, for the case of $r_2/r_1 = 2.09$ with both walls unwetted

$\frac{r-r_1}{r_2-r_1}$	ε_H measured at $Re = 96000$; ε_M measured at $Re = 93000$	ε_H measured at $Re = 140000$; ε_M measured at $Re = 137000$	ε_H measured at $Re = 199000$; ε_M measured at $Re = 195000$	ε_H measured at $Re = 285000$; ε_M measured at $Re = 281000$	ε_H measured at $Re = 382000$; ε_M measured at $Re = 377000$
0.050	0.72	0.73	0.75	0.79	0.79
0.075	0.75	0.78	0.78	0.85	0.87
0.100	0.77	0.82	0.84	0.90	0.93
0.150	0.81	0.85	0.85	0.91	0.95
0.200	0.84	0.88	0.87	0.90	0.92
0.300	0.94	0.96	0.97	0.97	0.96
0.400	(1.09)	(1.10)	(1.06)	(1.07)	(1.05)
0.500	0.92	0.95	0.98	0.99	(1.01)
0.600	0.82	0.81	0.79	0.84	0.87
0.700	0.79	0.78	0.78	0.80	0.82
0.800	0.78	0.79	0.80	0.82	0.85
0.900	0.75	(0.84)	(0.90)	—	—

Table 2. Present experimental values of ε_H divided by theoretical values of ε_M as predicted by Kays and Leung [4], for the case of $r_2/r_1 = 2.09$ with both walls unwetted

$\frac{r-r_1}{r_2-r_1}$	$Re = 96000$	$Re = 140000$	$Re = 199000$	$Re = 285000$	$Re = 382000$
0.050	0.75	0.77	0.80	0.83	0.88
0.075	0.82	0.83	0.87	0.91	1.00
0.100	0.85	0.86	0.91	0.97	(1.04)
0.150	0.90	0.90	0.92	1.00	(1.05)
0.200	0.93	0.93	0.95	0.98	(1.03)
0.300	0.89	0.89	0.93	0.96	1.00
0.400	0.90	0.91	0.96	(1.01)	(1.04)
0.431*					
0.500	0.83	0.85	0.90	0.96	(1.02)
0.600	0.85	0.83	0.85	0.90	0.97
0.700	0.88	0.85	0.87	0.91	0.96
0.800	0.87	0.87	0.90	0.94	0.99
0.900	0.61	0.84	(0.92)	—	—
$\bar{\psi}_1$ according to equation (7)	0.85	0.90	0.94	0.96	0.97

*At r_m.

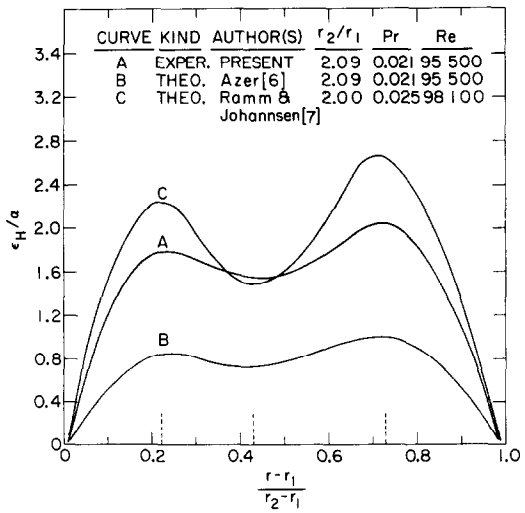

FIG. 10. Comparison of present results for the case of $r_2/r_1 = 2.09$ (both walls unwetted) with theoretical predictions by the methods of Azer [6] and Ramm and Johannsen [7].

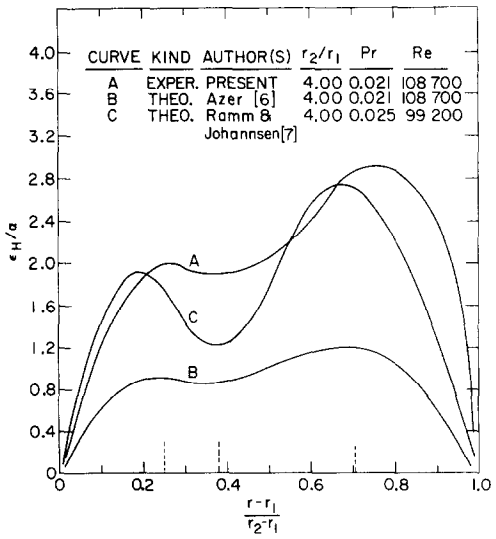

FIG. 11. Comparison of present results for the case of $r_2/r_1 = 4.00$ (both walls unwetted) with theoretical predictions by the methods of Azer [6] and Ramm and Johannsen [7].

Table 3. Present experimental values of ε_H divided by theoretical values of ε_M as predicted by Kays and Leung [4], for the case of $r_2/r_1 = 4.00$ with both walls unwetted

$\frac{r-r_1}{r_2-r_1}$	$Re = 109\,000$	$Re = 168\,000$	$Re = 233\,000$	$Re = 342\,000$	$Re = 474\,000$
0.050	0.65	0.68	0.72	0.75	0.78
0.075	0.69	0.72	0.75	0.77	0.82
0.100	0.70	0.76	0.78	0.81	0.85
0.150	0.80	0.82	0.84	0.88	0.91
0.200	0.85	0.87	0.90	0.94	0.96
0.300	0.90	0.95	0.98	(1.03)	(1.03)
0.380*					
0.400	0.88	0.94	0.98	(1.01)	(1.02)
0.500	0.86	0.90	0.93	0.98	0.99
0.600	0.90	(1.03)	0.98	(1.04)	(1.06)
$\bar{\psi}_1$ according to equation (7)	0.87	0.92	0.95	0.97	0.98

*At r_m.

Table 4. Comparison of present $\varepsilon_H/\varepsilon_M$ results (unwetted walls) with theoretical predictions for essentially the same Reynolds and Prandtl numbers for fully developed flow in concentric annuli

	Experimental	Theoretical		
	Present study	Azer [6]	Ramm and Johannsen [7]	
r_2/r_1	4.00	4.00	1.00	8.00
Re	474 000	474 000	470 000	470 000
Pr	0.0216	0.0216	0.025	0.025
$\frac{r-r_1}{r_2-r_1}$	$\varepsilon_H/\varepsilon_M$	$\varepsilon_H/\varepsilon_M$	$\varepsilon_H/\varepsilon_M$	$\varepsilon_H/\varepsilon_M$
0.050	0.78	0.48	0.92	0.92
0.075	0.82	0.52	0.93	0.92
0.100	0.85	0.54	0.93	0.92
0.150	0.91	0.57	0.94	0.93
0.200	0.96	0.58	0.95	0.93
0.300	(1.03)	0.58	0.95	0.93
0.400	(1.02)	0.58	0.95	0.96
0.500	0.99	0.60	0.95	0.98
0.600	(1.06)	0.61	0.95	0.98
0.700		0.61	0.95	0.97
0.800		0.60	0.94	0.96
0.900		0.55	0.93	0.94
0.950		0.47	0.91	0.91

0.48, 0.52 and 0.56 at $Re = 96\,000$, 140 000, 199 000, 285 000 and 382 000, respectively, for the same experimental conditions as those represented in Table 2.

In Tables 1 and 2, the results for $(r-r_1)/(r_2-r_1) = 0.900$ at the higher Reynolds numbers are obviously too high, since ε_M/ν should fall rapidly as either the inner or outer wall is approached. However, for the common case of heat transfer from the inner wall, the magnitude of ε_H in the radial region near the outer wall would have a negligible effect on the calculated heat-transfer coefficient. The values in parentheses in Tables 1 and 2 are theoretically too high.

Calculated $\varepsilon_H/\varepsilon_M$ results for the case $r_2/r_1 = 4.00$ with both walls unwetted are shown in Table 3. They are lower in the inner portion and higher in the outer portion of the annulus than the results in Table 2 for $r_2/r_1 = 2.09$. The method of Ramm and Johannsen also predicts a similar trend, but an extremely slight one (see Table 4). Both Azer's and Ramm and Johannsen's methods actually predict no significant effect on $\varepsilon_H/\varepsilon_M$ when r_2/r_1 is increased from 2.09 to 4.00, other things being equal. Table 4 shows a comparison between the present experimental results and the theoretical predictions of Azer [6] and Ramm and Johannsen [7] for a Reynolds number of $\sim$470 000. The Ramm and Johannsen results were read from Fig. 5 in their paper. They show little effect of r_2/r_1. It is clear that the present experimental results are much closer to those predicted by the method of Ramm and Johannsen than to those predicted by the method of Azer. However, from Table 4, we see that the $\varepsilon_H/\varepsilon_M$ profile as predicted by the method of Ramm and Johannsen is flatter than either that obtained in the present study or that predicted by the method of Azer.

No experimental values of $\varepsilon_H/\varepsilon_M$ for $(r-r_1)/(r_2-r_1) > 0.600$ are shown in Tables 3 and 4, because they were

all appreciably greater than 1.00. This is due to the fact that the ε_H profile in the region near the outer wall was too steep (see Fig. 11). As explained earlier, in the present study, the ε_H profiles in the vicinity of the outer wall are subject to appreciable error because of the flatness of the temperature profiles in that region.

The $\varepsilon_H/\varepsilon_M$ results for those cases where either one wall was, or both walls were, wetted will be summarized in [8], in connection with the presentation of Nusselt numbers.

5. DISCUSSION OF RESULTS

As far as we know, this is the first experimental study in which a liquid metal was flowed through an annulus and velocity and temperature profiles measured under the same conditions, so that ε_H profiles could be obtained. We therefore have no other experimental results with which the present ones can be compared. We can, however, make comparisons with predictions based on the theoretical methods of Azer [6] and Ramm and Johannsen [7]. It is possible to make two sets of comparisons based on our two cases where both walls were unwetted, for, as already mentioned, the hydrodynamic behavior of these cases was found to be very similar to those for ordinary liquids [1]. These comparisons are made in Figs. 10 and 11.

Figure 10 shows the results for the 2.09 annulus. Curve *A* is taken from Fig. 5. The differences between *Pr* and *Re* for curves *A* and *B* on the one hand and those for curve *C* on the other are not sufficiently great to prevent a valid comparison. The information for calculating curve *C* was taken from Fig. 8 in [7]. As far as magnitude is concerned, the three curves in Fig. 10 show little agreement. The experimental curve lies more or less between the two theoretical ones, but considerably closer to the Ramm and Johannsen curve than to the Azar curve. However, the Ramm and Johanssen curve shows a much deeper valley in the region of r_m than does the experimental curve. In this respect, the experimental curve agrees with the Azer curve. Moreover, we feel that our ε_H results in the radial range between the two maxima should be more accurate than in any other region, because the slopes of the temperature-profile curve in that range are neither very high nor very low. Thus, the present results suggest that the valley in curve *C* is too deep.

In certain other respects, the shapes of the three curves in Fig. 10 have much in common. They all have their maxima and minima at the same radial locations. The maxima in the inner portion come at the same radial position as the maximum in the measured ε_M profile. The same is true of the maxima in the outer portion. And the minima come at r_m, the observed radius of maximum velocity. These facts clearly show a fundamental relationship between ε_H and ε_M. However, in the present study, the valleys in the ε_H/α profiles were found to be considerably more shallow than those in the ε_M/ν profiles [1]; but we should remember that in the region or r_m, the accuracy of the former is much greater than that of the latter.

The general agreement between the three curves in Fig. 11 is no better than that in Fig. 10. Curves *A* and *C* agree moderately well up to an $(r-r_1)/(r_2-r_1) = 0.2$. Curve *A* is undoubtedly too high at the higher values of $(r-r_1)/(r_2-r_1)$, due to errors introduced by the very low slopes of the temperature profile in that radial region. The minima for all three curves occur at r_m. In the inner portion of the annulus, the maxima of curves *A* and *B* occur at the same radial location as the maximum in the ε_M profile [1], but the maximum in curve *C* falls appreciably to the left of that point. In the outer portion, the maxima for curves *B* and *C* occur at the same location as the maximum in the ε_M profile [1]. It would therefore appear that in radial region beyond $(r-r_1)/(r_2-r_1) = 0.7$, curve *C* is much more accurate than the other two. Regarding the steep valley in curve *C* in the region or r_m, the discussion on that topic in connection with Fig. 10 is also applicable here.

At this writing, a reliable method of predicting ε_H profiles for fully developed turbulent flow in concentric annuli remains to be established, but on the basis of the theoretical results obtained thus far and the corroborating evidence provided in the present study considerable progress has been made in achieving that goal.

In the fourth and final paper [8] on this project, Nusselt numbers for the various test conditions with the three different annuli will be presented, with special emphasis on the effect of wetting. These Nusselt numbers will be obtained from the original data in different ways and compared. Also, a recommended method of estimating $\varepsilon_H/\varepsilon_M$ ratios for use in theoretical heat transfer conditions for turbulent flow of liquid metals in annuli will be presented.

6. CONCLUSIONS

1. For a given radial position, ε_H was found to be either exactly or very nearly proportional to the flow rate, other things being equal.
2. The shapes of ε_H-vs-r profiles were found to be similar to the ε_M-vs-r profiles (see Fig. 10 in [1]), except in all cases the valleys of the ε_H curves in the region of the radius of maximum velocity were more shallow.
3. Each ε_H-vs-r profile shows a maximum in the inner portion of the annulus, a maximum in the outer portion, and a minimum at the radius of maximum velocity. The maxima apparently fall at the same radial locations as the corresponding maxima in the ε_M-vs-r profile.
4. Our ε_H results in the inner portion of an annulus are considerably more accurate than those in the outer portion, because of the lower slopes of the t-vs-r profiles in the outer portion, particularly in the proximity of the outer wall. To obtain more accurate ε_H data in the outer portions of annuli, the heat should be transferred from the outer wall.
5. The effect of wetting is illustrated in Fig. 9. When the inner wall only was wetted, the radius of maximum velocity shifted outward (compared to the

situation where neither wall was wetted), and this caused $(\varepsilon_{H1})_{max}$ to more nearly approach $(\varepsilon_{H2})_{max}$. When both walls were wetted, the radius of maximum velocity also moved outward (compared to the situation where neither wall was wetted) but not as far as in the situation where only the inner wall was wetted. This explains the relative positions of the three curves in Fig. 9.

6. Whereas $\varepsilon_H/\varepsilon_M$-vs-$r$ curves for ordinary fluids are concave upward for turbulent flow in annuli, those for liquid metals are concave downward. The $\varepsilon_H/\varepsilon_M$ is fairly uniform across the turbulent core but falls rapidly near each wall. There appears to be little influence of r_2/r_1 on the magnitude of $\varepsilon_H/\varepsilon_M$. However, it increases significantly with increase in Reynolds number.
7. Where nonwetting of the annulus walls occurs, the present ε_H radial profiles obtained with mercury give greater support to the theory of Ramm and Johannsen [7] than to that of Azer [6]. However, a typical Ramm and Johannsen profile for mercury shows a much deeper valley in the region of the radius of maximum velocity than do either the present results or the theory of Azer.

REFERENCES

1. P. J. Hlavac, B. G. Nimmo and O. E. Dwyer, Experimental study of effect of wetting on turbulent flow of mercury in annuli, *Int. J. Heat Mass Transfer* **15**, 2611–2631 (1972).
2. O. E. Dwyer, P. J. Hlavac and B. G. Nimmo, Effect of wetting on friction factors for turbulent flow of mercury in annuli, *J. Fluid Engng* **981**, 113–116 (1976).
3. M. W. Maresca and O. E. Dwyer, Heat transfer to mercury flowing inline through a bundle of circular rods, *J. Heat Transfer* **86**, 180–186 (1964).
4. W. M. Kays and E. Y. Leung, Heat transfer in annular passages—hydrodynamically developed turbulent flow with arbitrarily prescribed heat flux, *Int. J. Heat Mass Transfer* **6**, 537–557 (1963).
5. O. E. Dwyer, Eddy transport in liquid–metal heat transfer, *A.I.Ch.E. Jl* **9**, 261–268 (1963).
6. N. Z. Azer, The ratio of eddy diffusivities for heat and momentum transfer for fully developed turbulent flow in concentric annuli, *Proceedings of the 1970 Heat Transfer and Fluid Mechanics Institute*, pp. 15–31. Stanford University Press, Stanford, California (1970).
7. H. Ramm and K. Johannsen, Radial and tangential turbulent diffusivities of heat and momentum transfer in liquid metals, *Progress in Heat and Mass Transfer*, edited by O. E. Dwyer, Vol. 7, pp. 45–58. Pergamon Press, New York (1973).
8. B. G. Nimmo, P. J. Hlavac and O. E. Dwyer, Experimental study of heat transfer to mercury flowing turbulently in concentric annuli, To be published.

DIFFUSIVITE THERMIQUE TURBULENTE DANS LA DIRECTION RADIALE POUR UN ECOULEMENT TURBULENT DE MERCURE DANS UN ESPACE ANNULAIRE

Résumé—On a effectué une étude expérimentale sur les caractéristiques dynamiques et thermiques du mercure en écoulement turbulent établi dans un espace annulaire. Cet article, le troisième d'une série consacrée à ce projet, présente les résultats relatifs à la diffusivité turbulente de la chaleur. Les profils de vitesse et de température ont été mesurés dans un espace annulaire vertical avec transfert thermique sur une seule paroi, et les expériences ont été effectuées soit lorsque le mercure ne mouille pas du tout la paroi, soit lorsqu'il la mouille complètement.

La forme des profils de ε_H a été trouvé semblable à celle des profils de ε_M, les minima et les maxima se produisant à la même position radiale ou presque, dans ces conditions expérimentales identiques. Tous les minima se produisent au rayon du maximum de vitesse, mais les creux dans les profils de ε_H sont relativement moins profonds que ceux observés dans les profils de ε_M. L'effet du mouillage sur la forme relative des profils de ε_H, comme dans le cas des profils de ε_M, est appréciable. Lorsque aucune des deux parois n'est mouillée, le comportement hydrodynamique du mercure se trouve être [1] très comparable à celui des fluides ordinaires. Quoique les résultats présents, obtenus avec des parois non mouillées, ne soient pas en accord avec les prévisions basées sur la théorie actuelle, ils donnent un important appui en faveur de la méthode de Ramm et Johannsen [7].

DIE SCHEINBARE WÄRMELEITFÄHIGKEIT BEI RADIALEM WÄRMETRANSPORT IN TURBULENTEN QUECKSILBER-RINGSTRÖMUNGEN

Zusammenfassung—Es wurde eine grundlegende experimentelle Untersuchung des Strömungs- und Wärmeübergangsverhaltens von Quecksilber bei voll ausgebildeter, turbulenter Ringströmung durchgeführt.

Die vorliegende dritte Arbeit in einer Reihe von Arbeiten über dieses Projekt gibt die Ergebnisse über die scheinbare Wärmeleitfähigkeit wieder. Es wurden die Geschwindigkeits- und Temperaturprofile in vertikalen Ringspalten mit alleinigem Wärmeübergang am Innenzylinder gemessen. Die Versuche wurden mit teilweiser und vollständiger Benetzung der Kanalwände mit Quecksilber durchgeführt.

Die ε_H-Profile wiesen eine ähnliche Form wie die ε_M-Profile auf; unter denselben experimentellen Bedingungen erschienen die Maxima und Minima häufig nahe bei denselben oder an denselben radialen Stellen. Alle Minima traten in dem Radius auf, wo die Geschwindigkeit ein Maximum aufweist; die Täler in den ε_H-Profilen waren allerdings flacher als jene in den ε_M-Profilen. Bei beiden Profilen zeigte sich ein merklicher Einfluß der Benetzung auf die Form der Profile. Für den Fall, daß beide Wände unbenetzt sind, erwies sich das hydrodynamische Verhalten des Quecksilbers [1] als sehr änlich demjenigen üblicher Fluide. Obwohl die mit unbenetzten Wänden erhaltenen Ergebnisse nicht mit denjenigen nach vorhandenen Theorien vorausgesagten übereinstimmen, stützen sie deutlich die Methode von Ramm und Johannsen [7].

ТУРБУЛЕНТНАЯ ТЕМПЕРАТУРОПРОВОДНОСТЬ ПРИ РАДИАЛЬНОМ ТЕПЛОПЕРЕНОСЕ В ТУРБУЛЕНТНОМ ПОТОКЕ РТУТИ В КОЛЬЦЕВЫХ КАНАЛАХ

Аннотация — Проводилось исследование гидродинамических и теплопереносных характеристик потока ртути для случая полностью развитого турбулентного течения через кольцевые каналы. В этой статье, являющейся третьей в этом направлении, представлены результаты по турбулентной температуропроводности при теплопереносе. Проводилось измерение профилей скорости и температуры в вертикальных кольцевых каналах при переносе тепла только от внутренней стенки, причем в экспериментах стенки канала или совсем не смачивались, или же смачивались полностью. Найдено, что при одних и тех же экспериментальных условиях вид ε_H профилей аналогичен виду ε_M профилей с максимумами и минимумами, имеющими место при одинаковых или почти одинаковых значениях радиальной координаты. Все минимумы находились в области максимальной скорости, а «провалы» в ε_H профилях были относительно более мелкими, чем в ε_M профилях. Найдено, что, как в случае ε_M профиля, эффект смачивания существенно сказывается на виде ε_H профиля. Когда обе стенки не смочены, гидродинамическая картина потока ртути [1] была аналогична гидродинамике обычных жидсостей. Хотя результаты, полученные для случая несмачиваемых стенок, не согласуются с расчетами, основанными на известных методах, они подтверждают модель Рема и Йогансена.